

Research Letter

Kleinberg Navigation on Anisotropic Lattices

J. M. Campuzano, J. P. Bagrow, and D. ben-Avraham

Department of Physics, Clarkson University, Potsdam, NY 13699-5820, USA

Correspondence should be addressed to J. P. Bagrow, bagrowjp@gmail.com

Received 21 July 2008; Accepted 29 September 2008

Recommended by Peter McClintock

We study the Kleinberg problem of navigation in small-world networks when the underlying lattice is stretched along a preferred direction. Extensive simulations confirm that maximally efficient navigation is attained when the length r of long-range links is taken from the distribution $P(\mathbf{r}) \sim r^{-\alpha}$, when the exponent α is equal to 2, the dimension of the underlying lattice, regardless of the amount of anisotropy, but only in the limit of infinite lattice size, $L \rightarrow \infty$. For finite size lattices we find an optimal $\alpha(L)$ that depends strongly on L . The convergence to $\alpha = 2$ as $L \rightarrow \infty$ shows interesting power-law dependence on the anisotropy strength.

Copyright © 2008 J. M. Campuzano et al. This is an open access article distributed under the Creative Commons Attribution License, which permits unrestricted use, distribution, and reproduction in any medium, provided the original work is properly cited.

1. INTRODUCTION

The small-world phenomenon is one of the most intriguing properties of human society. This describes the fact that unrelated people in a society, who are a very large geographic distance apart from one another, tend to be connected by surprisingly short chains of acquaintances. This phenomenon was hypothesized in 1929 by Hungarian author Karinthy [1, 2] and was first observed experimentally in the 1960s with sociologist Stanley Milgram's seminal experiments [3], wherein randomly chosen people were selected to mail a letter to an unknown target person, but were only allowed to send the letter to a friend, who would pass the letter along to another friend, and so forth, until the target was reached. Successful transmissions took surprisingly few intermediate people, lending credibility to the turn of phrase "six degrees of separation," popularized by Karinthy. Understanding this phenomenon is an important sociological problem.

To study the underlying mechanism that led to Milgram's results, computer scientist Kleinberg modeled a society as follows [4, 5]. Begin with a large, regular square $L \times L$ lattice. Each node is connected to its nearest lattice neighbors and to a single random node a large distance away. The probability of nodes i and j being connected by such a long-range contact is

$$P_{ij}(\alpha) = \frac{r_{ij}^{-\alpha}}{\sum_{k \neq i} r_{ik}^{-\alpha}}, \quad (1)$$

where r_{ij} is the Euclidian distance between the two nodes

and the sum runs over all nodes in the network except i . Physically, the local lattice connections represent associations with immediate neighbors, fellow townspeople, and so forth, while long-range contacts might model friends or relatives in another city or country.

We seek to pass the message from a random starting node s to a random target t . Of great importance is the fact that each node has no information beyond the locations of its contacts and the target node t , so the operational algorithm must be *local* in character. Kleinberg has proved that no local algorithm can do better, functionally, than the *greedy* algorithm [4]: each message holder passes the message along to whichever of its contacts is closest to t , until the message reaches the target. Moreover, for $\alpha \neq 2$, the delivery time T (number of intermediate steps) scales as a *power* of L , while small-world behavior and the weakest dependence on lattice size emerges for $\alpha = 2$, where $T \sim \ln^2 L$.

The distribution of nodes on a regular square lattice is too rigid, failing to mimic important features of actual distributions of populations (or computer routers, etc.). In an effort to account for these, we have studied Kleinberg navigation in fractals [6], showing that the optimal long-contact exponent is then $\alpha = d_f$, the fractal dimension of the lattice. In this letter, we study the effects of anisotropy—another commonly encountered distortion of the ideal Kleinberg lattice. Our results indicate that in the limit of lattice size $L \rightarrow \infty$, the optimal contact exponent for two-dimensional lattices is still $\alpha = 2$. For finite L , we find an

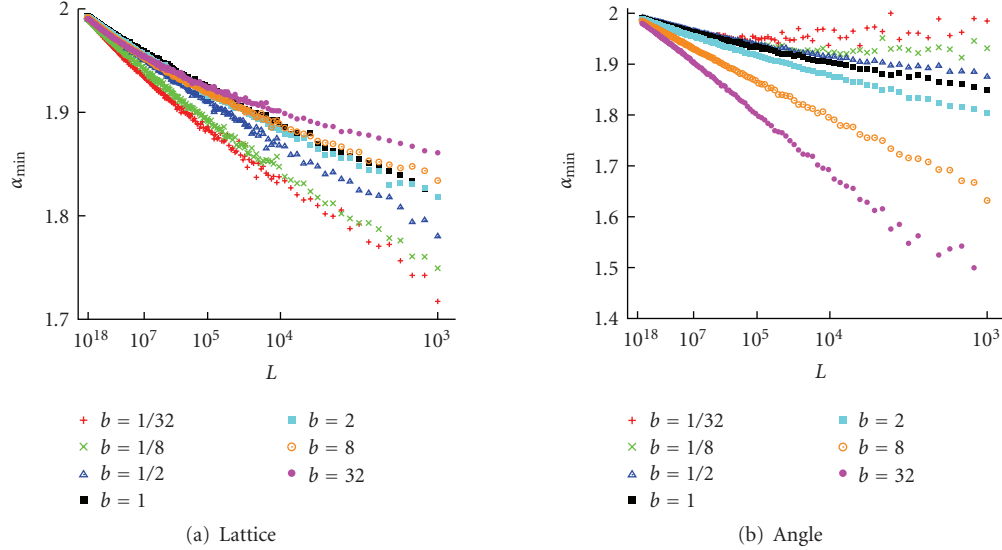


FIGURE 1: Simulations for lattice and angle anisotropies. A horizontal scale of $1/\ln^2 L$ is used throughout. All curves approach $\alpha(\infty)$, regardless of b . For the lattice case, there is a crossover effect where curves for $b > 1$ dip below the $b = 1$ curve. For the angular case, curves for $b > 1$ approach the infinite limit at differing rates, while curves for $b < 1$ eventually collapse onto the $b = 1$ curve. These phenomena are further explored in Figure 3. See Figure 2 for the extrapolated $\alpha(\infty)$.

optimal exponent $\alpha(L)$ quite different from the infinite limit. The convergence to $\alpha = 2$ as $L \rightarrow \infty$ shows interesting power-law dependence on the anisotropy strength.

2. ANISOTROPIC LATTICES

We wish to study the isolated effect of anisotropy on Kleinberg navigation. To do this, we begin with a regular square lattice ($d = 2$) and introduce one of two forms of anisotropy.

(i) *Lattice anisotropy*. The underlying lattice is stretched horizontally, along the x -axis, by a factor $b > 0$, such that the area of each cell goes from 1×1 to $b \times 1$.

(ii) *Angular anisotropy*. Long-range contacts are chosen preferably along the vertical direction by a factor $b > 0$. More precisely, the random angle θ of each long-range contact vector (measured counter-clockwise, from the x -axis) is modified to θ' :

$$\theta' = \arctan(b \tan \theta). \quad (2)$$

Both of these types of anisotropy tend to favor connections in the vertical y -direction if $b > 1$, and along the x -direction if $0 < b < 1$.

3. SIMULATIONS

To simulate Kleinberg navigation efficiently, we use several tricks and approximations. First, rather than testing a finite-size square $L \times L$ lattice, we consider an infinite lattice and place the source and target at distance L from one another. Since the message always progresses toward the target, by the greedy algorithm, the message holder remains within a disc of radius L centered on the target node, so in practice only a finite number of sites would be explored anyway. Second,

the computation of the normalizing sum in the denominator of (1) is dependent (in finite lattices) on the location of the node i , and can be very time-consuming. The infinite lattice circumvents this problem, as the normalizing constant is the same for all nodes. Note, however, that $\sum_k r_{ik}^{-\alpha}$ does not converge for $\alpha < d$. In that case, we imagine a lattice larger than the L -disc of activity, with periodic boundary conditions, such that the normalizing factor is still the same for all sites.

Because of the monotonic progression toward the target no site is ever revisited in the process. Moreover, as observed by Kleinberg [5], one can think of the long-contact link-out of node i as being created at the very instant that the message arrives at i . Thus, the full lattice is unnecessary, and we need keep in memory only the current location of the message holder (and the location of the target). When the message arrives at i , we create a random long contact, compare the distances of all five neighbors of i (the four lattice neighbors and the long contact) to the target, and move the message to the site closest to the target.

The long contact is created by choosing a random distance and angle, (r, θ) . In order to reproduce the correct $P(r_{ij}) \sim r_{ij}^{-\alpha}$, the distance r is taken from the distribution $P(r) \sim r^{-\alpha-1}$, to account for the linear growth of the area of the ring where the contact might fall. The angle θ is distributed uniformly between 0 and 2π . In the case of angular anisotropy, θ is replaced by θ' , according to (2). Finally, a vector (r, θ) is drawn from site i , and the contact is placed on the site j closest to the vector tip.

Because of the anisotropy, the angular displacement from the source to the target makes a difference. It is sufficient to test only the two extremes of $\theta = 0$ and $\theta = \pi/2$, where the target is either parallel or perpendicular to the anisotropy direction. We note, however, that anisotropy strength b and a target at $\theta = 0$ is equivalent to anisotropy $1/b$ and target at

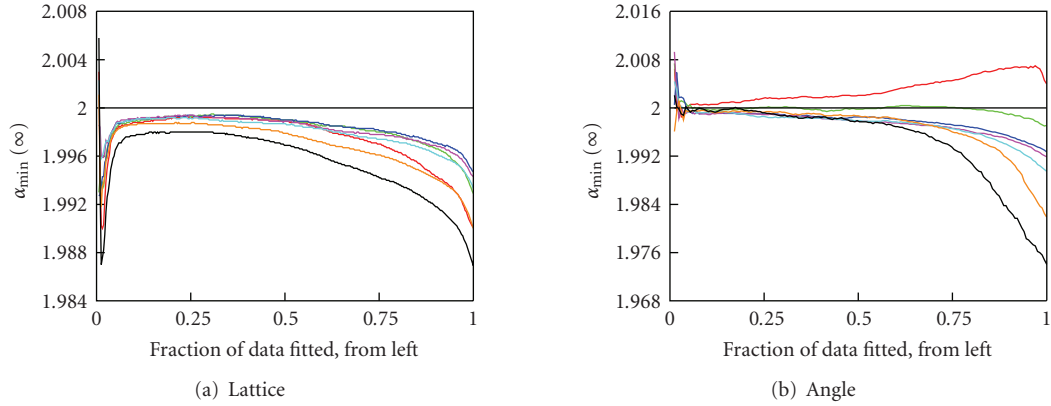


FIGURE 2: Extrapolation results for (a) lattice and (b) angular anisotropies. Extrapolating to $1/\ln^2 L \rightarrow 0$ with a linear least-squares fit to the curves in Figure 1 shows excellent convergence of $\alpha(\infty)$ to the expected value of $d = 2$. Good values should occur when the curves are flattest, which happens roughly around 0.25. A more robust fitting procedure could be used, but the accuracy of these results implies that it is unnecessary. The horizontal lines at $\alpha = 2$ provide a guide for the eye.

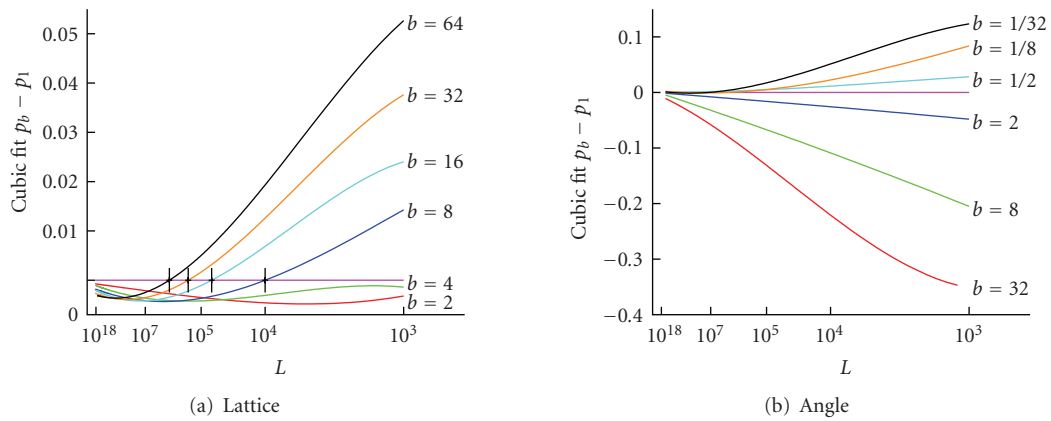


FIGURE 3: Curves relative to the isotropic divide $b = 1$, for (a) lattice and (b) angular cases. To provide a measure of smoothing, cubic polynomials p_b were fitted to the curves in Figure 1. To clarify the impact of anisotropy, we show the behavior relative to the isotropic case by subtracting p_1 from each p_b . This maps the isotropic curve to a horizontal line and introduces only minor distortion. The crossover behavior for $b > 1$ is clearly displayed.

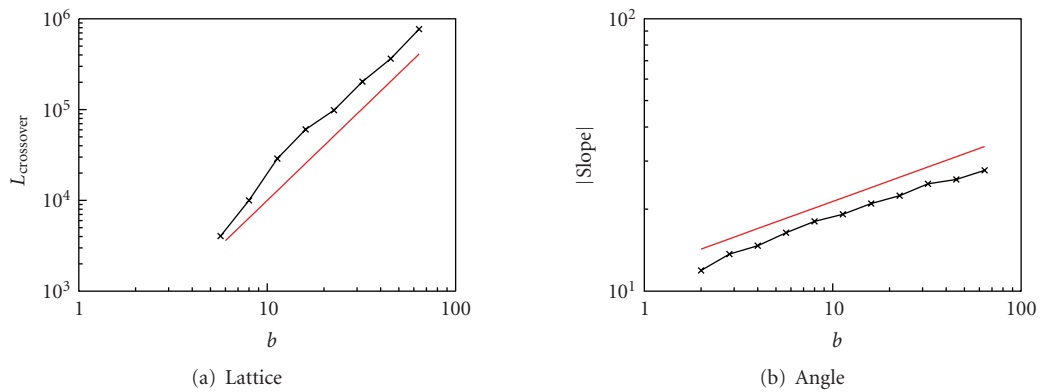


FIGURE 4: Dependence of results on anisotropy strength b for (a) lattice and (b) angular anisotropies. The straight lines are of slopes 2 and $1/4$, respectively.

$\theta = \pi/2$. For this reason, we simply set the source and target at $(0, 0)$ and $(L, 0)$, respectively, throughout, and let b vary both below and above the isotropic divide of $b = 1$.

Simulations were performed for various values of b over a large range of α and L , each averaged 1000 times. For each b and L , the minimum α was computed by first fitting a fifth-order polynomial to the averaged data, then using Newton's Method on the polynomial's derivative. (A parabola could be fitted to the data closest to the minimum, but we must first know what is "closest." A higher-order polynomial overcomes this difficulty, similar to including higher order terms in a series expansion near the minimum of a function.) Finally, α_{\min} was plotted as a function of $1/\ln^2 L$ for each chosen value of b . These are shown in Figure 1 and indicate that $\alpha_{\min} \rightarrow 2$ as $L \rightarrow \infty$, regardless of b . In Figure 2, we show detailed results of the extrapolation to $L \rightarrow \infty$.

To further clarify the behavior shown in Figure 1, the following procedure was performed. First, fit a cubic polynomial p_b , using least squares, to each b 's curve. Then, subtract that polynomial from the isotropic case, $p_b - p_1$. This maps $b = 1$ to the horizontal axis and gives the behavior of the $b \neq 1$ curves "relative" to the isotropic curve. These are shown in Figure 3. The different behavior for each type of anisotropy is clear: for both types of anisotropy, the results for $b > 1$ show dramatic differences from the isotropic case of $b = 1$ (the differences for $b < 1$ and large L are negligible). For lattice anisotropy, the $b > 1$ curves start above the $b = 1$ curve and cross below until they eventually converge at a similar rate, as $L \rightarrow \infty$. For the angular anisotropy, the $b > 1$ curves approach $\alpha(\infty)$ at a different rate than the $b = 1$ curve, resulting in distinctly different slopes in the plots of Figure 1(b).

The observed "crossover" behavior present in the lattice anisotropy is somewhat unexpected. The crossover point, $L_{\text{crossover}}(b)$, is explored by finding the zero of each $p_b - p_1$. These are plotted in Figure 4(a), and seem to indicate a power-law relationship, $L_{\text{crossover}}(b) \sim b^2$. Likewise, the different slopes for angular anisotropy, plotted in Figure 4(b), show power-law behavior and seem to increase roughly as $b^{1/4}$. What is responsible for these phenomena remains an open question.

4. CONCLUSIONS

We have shown, by extensive numerical simulations, that Kleinberg navigation in two-dimensional lattices with two types of anisotropy displays the same gross characteristics as navigation in isotropic lattices. In particular, the optimal long-contact exponent in the limit of infinitely distant source and target remains $\alpha = 2$, even in the presence of anisotropy.

It is worthwhile to note that the actual values for the optimal exponent $\alpha(L)$ for finite L can differ considerably from the limit $\alpha = 2$, even for reasonably large lattices. Thus, for practical applications, the optimal exponent ought to be evaluated on a case-by-case basis.

The modes of convergence to the limit $L \rightarrow \infty$ show intriguing power-law dependence upon the strength of the anisotropy. A theoretical explanation for this behavior remains the subject of future work.

APPENDIX

FINDING α_{\min}

The analysis of the simulations hinges upon finding the α with the smallest transit time T . Finding this value is difficult due to small fluctuations near the minimum, fluctuations which remain even after averaging. To overcome this, we simply fit a least-squares polynomial curve to the data, providing an additional degree of smoothing and interpolation. Since the exact location of the minimum is unknown, a quadratic polynomial may be skewed. Instead, we chose to fit a fifth-order polynomial and find the minimum using Newton's method on its derivative. Since all the minima are close to $\alpha = 2$, we choose this as our initial guess for Newton's method. Moreover, all the data shown in the preceding figures had clean fits.

ACKNOWLEDGMENTS

The authors gratefully acknowledge NSF Award PHY0555312 for partial funding for D. ben-Avraham, and the support of an NSF Graduate Research Fellowship for J. P. Bagrow. J. M. Campuzano has been supported as a Summer Research Undergraduate Student by the McNair Program at Clarkson University.

REFERENCES

- [1] A.-L. Barabási, *Linked: How Everything is Connected to Everything Else and What It Means for Business, Science, and Everyday Life*, Plume, New York, NY, USA, 2003.
- [2] F. Karinthy, "Chains," in *Everything is Different*, Atheneum Press, Budapest, Hungary, 1929.
- [3] S. Milgram, "The small-world problem," *Psychology Today*, vol. 1, no. 1, pp. 61–67, 1967.
- [4] J. M. Kleinberg, "Navigation in a small world," *Nature*, vol. 406, no. 6798, p. 845, 2000.
- [5] J. M. Kleinberg, "The small-world phenomenon: an algorithm perspective," in *Proceedings of the 32nd Annual ACM Symposium on Theory of Computing (STOC '00)*, pp. 163–170, Portland, Ore, USA, May 2000.
- [6] M. R. Roberson and D. ben-Avraham, "Kleinberg navigation in fractal small-world networks," *Physical Review E*, vol. 74, no. 1, Article ID 017101, 3 pages, 2006.

Special Issue on Robotic Astronomy

Call for Papers

The number of automatic astronomical facilities worldwide continues to grow, and the level of robotisation, autonomy, and networking is increasing as well. This has a strong impact in many astrophysical fields, like the search for extrasolar planets, the monitoring of variable stars in our galaxy, the study of active galactic nuclei, the detection and monitoring of supernovae, and the immediate follow-up of high-energy transients such as gamma-ray bursts.

The main focus of this special issue will be on the new and existing astronomical facilities whose goal is to observe a wide variety of astrophysical targets with no (or very little) human interaction. The special issue will become an international forum for researchers to summarize the most recent developments and ideas in the field, with a special emphasis given to the technical and observational results obtained within the last five years. The topics to be covered include, but not limited to:

- Robotic astronomy: historical perspective
- Existing robotic observatories worldwide
- New hardware and software developments
- Real-time analysis pipelines
- Archiving the data
- Telescope and observatory control systems
- Transient detection and classification
- Protocols for robotic telescope networks
- Standards and protocols for transient reporting
- Scientific results obtained by means of robotic observatories
- Global networks
- Future strategies

Before submission authors should carefully read over the journal's Author Guidelines, which are located at <http://www.hindawi.com/journals/aa/guidelines.html>. Authors should follow the Advances in Astronomy manuscript format described at the journal site <http://www.hindawi.com/journals/aa/>. Prospective authors should submit an electronic copy of their complete manuscript through the journal Manuscript Tracking System at <http://mts.hindawi.com/> according to the following timetable:

Manuscript Due	June 15, 2009
First Round of Reviews	September 15, 2009
Publication Date	December 15, 2009

Lead Guest Editor

Alberto J. Castro-Tirado, Instituto de Astrofísica de Andalucía, P.O. Box 03004, 18080 Granada, Spain; ajct@iaa.es

Guest Editors

Joshua S. Bloom, Astronomy Department, University of California, Berkeley, CA 94720, USA; jbloom@astro.berkeley.edu

Lorraine Hanlon, School of Physics, University College Dublin, Belfield, Dublin 4, Ireland; lorraine.hanlon@ucd.ie

Frederic Hessman, Institut für Astrophysik, Georg-August-Universität, Friedrich-Hund-Platz 1, 37077 Göttingen, Germany; hessman@astro.physik.uni-goettingen.de

Taro Kotani, Department of Physics and Mathematics, Aoyama Gakuin University, 5-10-1 Fuchinobe, Sagamihara, Kanagawa 229-8558, Japan; kotani@hp.phys.titech.ac.jp

Special Issue on Gauge/String Duality

Call for Papers

The subject of gauge/string duality has made rapid strides in recent years. The best known example of this duality is the conjecture that Type II B string theory in $AdS_5 \times S^5$ with N units of R-R five form flux is dual to $\mathcal{N} = 4$ theory in $d = 4$ with gauge group $SU(N)$. Since then this conjecture has given new insight into both gauge theory and string theory. More recently attempts have been made to expand its reach to include more realistic theories in the same universality class as QCD. Considering the volume of work in the literature, the guest editors are of the opinion that now is an appropriate time to bring out a Special Issue containing articles covering diverse aspects of gauge/string duality. We invite contributions on all aspects of gauge/string duality. As a rough guide, we encourage articles in the following areas:

- Holographic duals of QCD-like theories
- Holographic description of transport phenomena, symmetry breaking, quark-gluon plasma, and phase transitions
- AdS_4/CFT_3
- Nonrelativistic AdS/CFT . Applications in condensed matter physics
- Holographic models for Cosmology of early Universe
- Integrable structures in AdS/CFT

The submission of review articles describing developments in the past five to six years is highly encouraged, but also original research contributions will be considered.

Before submission authors should carefully read over the journal's Author Guidelines, which are located at <http://www.hindawi.com/journals/ahep/guidelines.html>. Prospective authors should submit an electronic copy of their complete manuscript through the journal Manuscript Tracking System at <http://mts.hindawi.com/> according to the following timetable:

Manuscript Due	December 1, 2009
First Round of Reviews	March 1, 2010
Publication Date	June 1, 2010

Lead Guest Editor

Kadayam S. Viswanathan, Department of Physics and IRMACS, Simon Fraser University, Burnaby, BC, Canada V3C3R8; kviswana@sfu.ca

Guest Editors

Wolfgang Mück, Dipartimento di Scienze Fisiche, Università degli Studi di Napoli Federico II and INFN, Sezione di Napoli, Via Cintia, 80126 Napoli, Italy; wolfgang.mueck@na.infn.it

Carlos Nunez, Department of Physics, University of Wales Swansea, Singleton Park, Swansea SA2 8PP, UK; c.nunez@swan.ac.uk

Leopoldo A. Pando Zayas, Michigan Center for Theoretical Physics, The University of Michigan, Ann Arbor, MI 48109-1120, USA; pandoz@umich.edu

Alfonso V. Ramallo, Departamento de Física de Partículas, Universidade de Santiago de Compostela and Instituto Galego de Física de Altas Energías (IGFAE), E-15782 Santiago de Compostela, Spain; alfonso@fpaxp1.usc.es

Radoslav C. Rashkov, Department of Physics, Sofia University, 5 J. Bourchier Boulevard, 1164 Sofia, Bulgaria; Institute for Theoretical Physics, Vienna University of Technology, Wiedner Hauptstr. 8-10, 1040 Vienna, Austria; rash@hep.itp.tuwien.ac.at

Soo-Jong Rey, School of Physics and Astronomy, Seoul National University, Gwanak Campus Bldg 27 Room 209, Seoul, South Korea; sjrey@snu.ac.kr